

Interplay between Raman and polarization effects in next-generation passive optical networks

M. Cantono,¹ V. Curri,¹ A. Mecozzi² and R. Gaudino^{1,*}

¹DET, Politecnico di Torino, Corso Duca degli Abruzzi, 24, 10129, Torino, Italy

² Department of Physical and Chemical Sciences, University of L'Aquila, via Vetoio 1, 67100, L'Aquila, Italy

[*roberto.gaudino@polito.it](mailto:roberto.gaudino@polito.it)

Abstract: In this paper, we study in details some Raman-induced impairments that arise in Next-Generation Passive Optical Networks (NG-PON2) in a full coexistence scenario between GPON and TWDM-PON. The main new contribution of this paper is to take into account the polarization launches of the different signals at the transmitter, in order to find the best polarization arrangement. We found that launching the TWDM-PON wavelengths on alternately orthogonal polarization minimizes the Raman depletion effect on GPON over all possible PMD values, thus resulting in the optimal polarization launching condition, while any other polarization launch has a higher out of service probability for realistic PMD values.

© 2015 Optical Society of America

OCIS codes: (060.0060) Fiber optics and optical communications; (060.4510) Optical communications; (060.4370) Nonlinear optics, fibers.

References and links

1. ITU-T Recommendation G.989.1 “40-Gigabit-capable passive optical networks (NG-PON2)”
2. G. Simon, F. Saliou, P. Chanclou, B. Le Guyader and L. Guillo “Stimulated Raman Scattering Impairments Induced by NGPON2 Introduction in Co-existing PONs,” in *Optical Fiber Communication Conference*, OSA Technical Digest (online) (Optical Society of America, 2015), paper Th2A.52. Los Angeles (US) - March 23-27, 2015
3. V. Curri, S. Capriata, and R. Gaudino, “Outage probability due to Stimulated Raman Scattering in GPON and TWDM-PON coexistence,” in *Optical Fiber Communication Conference*, OSA Technical Digest (online) (Optical Society of America, 2014), paper M31.2. San Francisco (US) - March 9-13, 2014
4. ITU-T Recommendation G.989.2, Appendix “Nonlinear Raman Interactions in Optical Fibers and Mitigation Technologies for Coexistence of Multiple PON Systems”.
5. Q. Lin and G. Agrawal, “Vector theory of stimulated Raman scattering and its application to fiber-based Raman amplifiers,” *J. Opt. Soc. Am. B* **20** (8), 1616–1631 (2003).
6. E. S. Son, J. H. Lee, and Y. C. Chung, “Statistics of Polarization-Dependent Gain in Fiber Raman Amplifiers,” *J. Lightwave Technol.* **23** (3), 1219–1226 (2005)
7. C. D. Poole and D. L. Favin, “Polarization-Mode Dispersion Measurements Based on Transmission Spectra Through a Polarizer,” *J. Lightwave Technol.* **12** (6), 917–929 (1994)
8. D. Marcuse, C. R. Menyuk, and P. K. A. Wai, “Application of the Manakov-PMD equation to studies of signal propagation in optical fibers with randomly varying birefringence,” *J. Lightwave Technol.* **15** (9), 1735–1746 (1997)
9. ITU-T Recommendation G.984.2 “Gigabit-capable Passive Optical Networks (GPON): Physical Media Dependent (PMD) layer specification”

1. Introduction

In this paper we investigate on a problem that recently arose during the definition of the new standard for Next-Generation Passive Optical Networks (NG-PON2, see ITU-T 989 Recommendation [1]), related to the fact that in a full coexistence scenario the N_{TWDM} wavelengths for the new Time and Wavelength Division Multiplexed PON (TWDM-PON) channels may deplete the lower wavelength GPON channel due to nonlinear Raman effects along the PON fiber. As demonstrated in recent experiments [2], this situation is potentially critical in NG-PON2 for two joined reasons: (i) the new TWDM-PON channels are specified to have very high power for the downstream (DS) launch, with values above 9 dBm per wavelength, so that the aggregated power of the N_{TWDM} wavelengths is sufficiently high to create a significant Raman nonlinearity and (ii) the system margin specified for the “legacy” GPON is very low, and thus even a fraction of dB depletion on GPON due to this effect can in some situations make the GPON channel go out of service. A similar situation holds for the TWDM-PON interactions with XG-PON and RF-Video but they are not treated in this paper for space limitations. The only relevant difference for these interactions is related to the efficiency of the Raman effect that will be lower than the GPON and TWDM-PON case, whereas the methodology used here remains still valid also in the other situations.

This paper extends the results we preliminary presented in [3] by giving a much more complete analysis on the outage probability evaluation and on the best possible polarization launch solutions at the transmitter. In particular, in our previous paper [3] we assumed the input state of polarization (SOP) of each channel to be uniformly distributed over the Poincaré sphere. Such hypothesis allowed a closed analytical formulation of the statistics of the Stimulated Raman Scattering (SRS) depletion on GPON, but did not allow to look for the best polarization launching condition. The goal of this paper is thus the extension of the previous analysis to scenarios in which the input SOP are known and deterministic. This target is of practical interest in order to define an optimal launching scheme able to minimize SRS depletion. In particular, we believe it is very important to give a theoretical support to some of the empirical guidelines that ITU-T Recommendation 989.2 has given for this physical layer impairment in an Appendix [1]. Moreover, the paper also give some new empirical formulas for the maximum acceptable power on the TWDM-PON channels.

Unfortunately the intricate stochastic nature of the problem prevents a complete characterization of the probability density function of the SRS depletion depending on input Stokes vectors. To overcome such limitation we implemented a Monte-Carlo simulation software able to emulate the evolution of the SOP of the wavelengths of interests along the fiber, and compute the Raman depletion on the wavelength of interest.

The paper is organized as follows. In Sec. 2 we present the system scenario, and we give the mathematical tools to analyze the problem. Then, in Sec. 3 we give the definition of outage probability for the GPON channel as a function of the transmitted power per TWDM-PON channel P_{TWDM} , and we present the obtained numerical results, discussing on the best polarization launches. Then Sec. 4 proposes some heuristic fitting functions to estimate the maximum allowed power P_{TWDM} to keep the out of service probability on GPON under reasonable level, then we give in the final Sec. 5 some practical design rules and system discussions.

2. System scenario

We consider a realistic NG-PON2 system scenario characterized by a GPON signal at 1490 nm coexisting with N_{TWDM} TWDM-PON wavelengths placed in the L-Band around 1600 nm. For the Raman effect analysis that is the focus of this paper, we may assume that what counts is the average power on each of these wavelengths, which thus for the Raman study can be assumed to be continuous wave (CW), thanks to the strong walk-off effect generated by chromatic dis-

persion on SMF fibers (which are the only types of fiber used in PON [1]) that averages out the instantaneous power variation due to the digital On-Off Keying (OOK) modulation that is present on each wavelength. The GPON channel and each TWDM-PON channel average input power are indicated as P_{GPON} and P_{TWDM} , respectively. As extensively shown in Raman amplifier literature [5, 6], polarization mode dispersion (PMD) randomly rotates the SOP of the involved wavelengths, generating stochastic Raman gain and pump depletion variations. In the considered NG-PON2 scenario, it turns out that depletion on GPON is the most relevant effect, as it corresponds to random depletion on the (relatively weak) GPON wavelength caused by nonlinear power transfer to (much stronger) TWDM-PON channels. It can be shown [3, 6] that the Raman depletion in dB units is given by:

$$A_{GPON}^{dB} = 10 \log_{10}(e) C_r(\Delta\omega) P_{TWDM} L_{eff} \sum_i^{N_{TWDM}} [1 + \eta_i(L)] \quad [\text{dB}] \quad (1)$$

where L is the PON SMF fiber length and

$$\eta_i(L) = \frac{1}{L_{eff}} \int_0^L [\hat{\mathbf{s}}_{GPON}(z) \cdot \hat{\mathbf{s}}_{TWDM_i}(z)] \exp(-\alpha z) dz, \quad (2)$$

$L_{eff} = [1 - \exp(-\alpha L)] / \alpha$ is the fiber effective length, α [1/km] is the fiber loss coefficient, $C_r(\Delta\omega)$ [1/mW/km] represents the polarization-average Raman efficiency at $\Delta\omega$, i.e. the spectral distance between GPON and TWDM-PON wavelengths. $C_r(\Delta\omega)$ is assumed to be constant for all TWDM-PON channels. Finally $\hat{\mathbf{s}}_{GPON}(z) \cdot \hat{\mathbf{s}}_{TWDM_i}(z)$ is the scalar product of the Stokes vectors of GPON and TWDM-PON signals, respectively. From Eq. (1) we observe that A_{GPON}^{dB} is a random variable whose random nature depends only on $\eta_i(L)$ and whose values span from 0 dB (in the unlikely event that $\hat{\mathbf{s}}_{GPON}(z)$ and $\hat{\mathbf{s}}_{TWDM_i}(z)$ are orthogonal along the full fiber length) to $A_{max}^{dB} = 20 \log_{10}(e) C_r(\Delta\omega) P_{TWDM} L_{eff} N_{TWDM}$ dB (in the again unlikely event that $\hat{\mathbf{s}}_{GPON}(z)$ and $\hat{\mathbf{s}}_{TWDM_i}(z)$ are perfectly aligned along the full fiber length). The random nature of the problem, due to the structure of the $\eta_i(L)$ formula, thus depends on the polarization launching conditions $\hat{\mathbf{s}}_{GPON}(0)$ and $\hat{\mathbf{s}}_{TWDM_i}(0)$ and on their random evolution along the fiber due to PMD. In our previous paper [3] we assumed that the input SOP of both GPON and TWDM-PON were uniformly distributed over the Poincaré sphere, obtaining a sort of “averaging” of the problem over all possible input polarizations. Under these condition, we showed in [3] that the probability density function (PDF) of $\eta(L)$ is Gaussian with known average value and variance. These hypotheses are anyway not realistic in an NG-PON2 transmitter, where no polarization scrambling devices are (for the moment) assumed by the ITU-T standard. We thus extend in this paper our previous work to generic but deterministic input states of polarization. This apparently minor detail is actually very relevant, since it will allow in the following Sections to discuss on the best polarization launch conditions.

Unfortunately, for deterministic input SOP an analytical formulation of the problem is not available, since also the original papers we used in our analysis [5, 6] make uses of some input “averaging” assumptions. Consequently, we resorted in this paper to very detailed Monte Carlo analyses of PMD effects to derive the PDF of the SRS-induced depletion $f(A_{GPON}^{dB})$, that then enables to evaluate the possible SRS-induced outage probability. The fiber emulator we used is based on the well-known coarse step method [7, 8], also indicated as the waveplate model, which approximates the continuous birefringence variations of a realistic fiber by the concatenation of fixed length birefringent *plates*, each of them characterized by a random orientation of its principal states of polarization (PSP) and a given differential group delay (DGD) that is determined by:

$$\Delta\tau_p = \sqrt{\frac{3\pi}{8}} \delta_{PMD} \sqrt{L_p} \quad (3)$$

where L_p is the length of each section. L_p is chosen to be larger-equal than the correlation length of the fiber birefringence, that is typically of the order of few hundreds of meters. We run extremely lengthy numerical simulations over the equivalent of 1.5×10^7 random realization of the PON fiber to reasonably span also the tails of the resulting random distribution.

3. Outage probability: definition and results

As we already introduced in [3], we believe that a very important system parameter to be analyzed in the scenario of this paper is the outage (or out-of-service) probability on the GPON channel, defined as the probability that the SRS-induced depletion A_{GPON}^{dB} is larger than a given threshold μ_{SRS}^{dB} . Hence, the outage probability of the GPON channel due to the SRS is defined as $P_{OOS} = P\{A_{GPON}^{dB} > \mu_{SRS}^{dB}\}$. The standard for GPON (Recommendation ITU-T G.984.2 [9]) defines in its clause 8.2.8.3 a parameter called ‘‘Maximum optical path penalty’’ and specifies it to be equal to 1 dB. To fix a reasonable value, we have thus tentatively set $\mu_{SRS}^{dB}=1$ dB to the SRS-induced GPON extra loss.

In order to normalize the problem to the transmitted power, we observe in Eq. (1) that A_{GPON}^{dB} scales linearly with P_{TWDM} expressed in mW, so that we can write $A_{GPON}^{dB} = A_{GPON}^{0dBm} \cdot P_{TWDM}$, where A_{GPON}^{0dBm} is the SRS-induced depletion calculated for $P_{TWDM} = 1$ mW. Consequently, the outage probability can be expressed as:

$$P_{OOS} = P\left\{A_{GPON}^{dB} > \mu_{SRS}^{dB}\right\} = P\left\{A_{GPON}^{0dBm} > \frac{\mu_{SRS}^{dB}}{P_{TWDM}^{mW}}\right\} \quad (4)$$

allowing computing only A_{GPON}^{0dBm} using the PMD emulator independently of P_{TWDM} , then easily scaling it with P_{TWDM} .

We focus our study on the following three input SOP configurations that are qualitatively described in Fig. 1:

1. Co-polarized configuration: the GPON channel and all the TWDM-PON channels are parallel in polarization
2. Orthogonal configuration: the set of TWDM-PON channels are still co-polarized, but the GPON channel is orthogonal to this polarization;
3. DoP0 configuration: the GPON channel is orthogonal in polarization with respect to all odd TWDM-PON channels, and parallel in polarization with respect to even ones, i.e., the TWDM channels are alternately set over two orthogonal SOP. Such configuration is proposed in a specific G.989.2 Appendix [4] and, since it generates a zero composite degree of polarization (DoP) on the TWDM-PON set, is indicated in the standard as the ‘‘DoP0 configuration’’. Such configuration can be further generalized, removing any constraints on the mutual polarization alignment between the TWDM-PON channels and the GPON one.

We assumed $\mu_{SRS}^{dB} = 1$ dB and evaluated P_{OOS} for link lengths $L \in \{5, 10, 20, 30, 40\}$ km, for eight PMD values $\delta_{PMD} \in [0.001, 0.1]$ ps/ $\sqrt{\text{km}}$ and for 4 or 8 TWDM-PON channels spaced 100 GHz around 1600 nm.

As a first output of our Monte-Carlo study, we obtained the resulting A_{GPON}^{dB} PDF for different values of PMD coefficient δ_{PMD} and input SOP configurations as shown in Fig. 2, and we discuss the results in the following subsections as a function of increasing values of PMD and power P_{TWDM} .

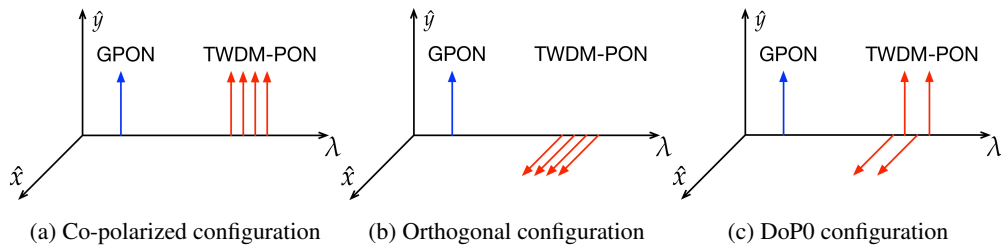


Fig. 1. Qualitative description of the three input SOP configurations we analyzed.

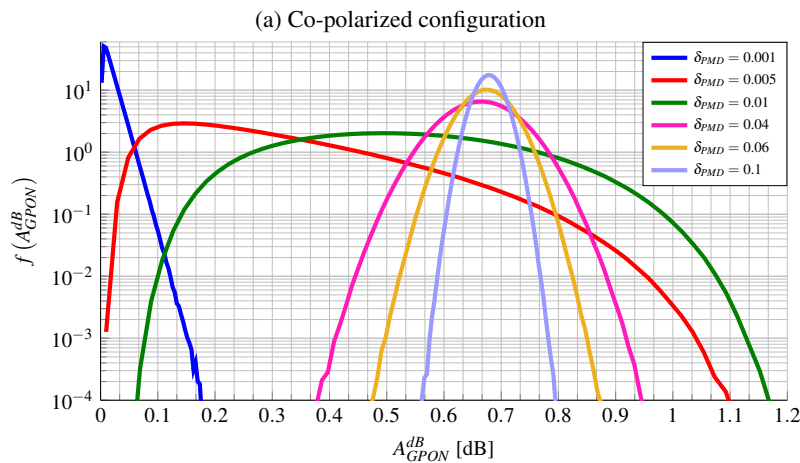
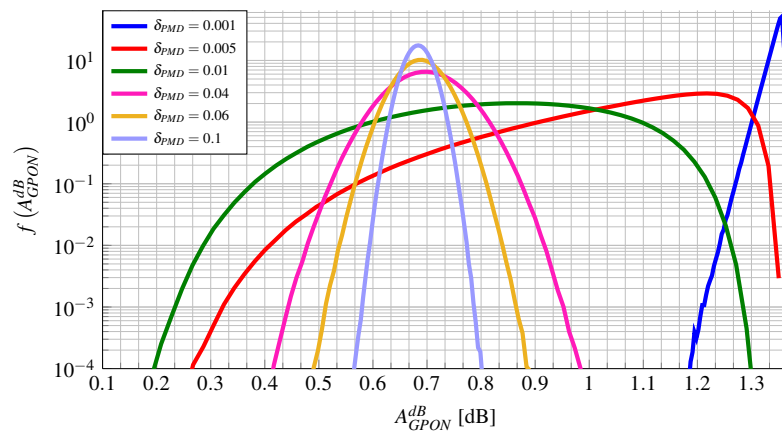


Fig. 2. Simulative A_{GPON}^{dB} PDF - $N_{TWDM} = 4$, $L = 20$ km, $P_{TWDM} = 10$ dBm. The DoP0 configuration is omitted, since for that configuration the PDF is a Dirac Delta centered in $\langle A_{GPON}^{dB} \rangle$

3.1. Co-polarized input SOP

For co-polarized input SOP (Fig. 2(a)) and extremely low PMD ($\delta_{PMD} \leq 0.001$ ps/ $\sqrt{\text{km}}$), the $f(A_{GPON}^{dB})$ PDF of the GPON depletion tends to be deterministic and close to the aforementioned maximum value A_{max}^{dB} dB, since for very low PMD the co-polarization condition tends to be preserved along the full fiber length. Therefore, in this case the outage probability is very steep and abruptly jumps from 0 to 1 as a function of P_{TWDM} for:

$$P_{TWDM} \geq \frac{1}{20 \log_{10}(e) C_r L_{eff} N_{TWDM}}. \quad [\text{mW}] \quad (5)$$

As PMD increases to more realistic values $\delta_{PMD} > 0.001$ ps/ $\sqrt{\text{km}}$, the $f(A_{GPON}^{dB})$ PDF spreads and its average value decreases, since SOPs are more and more scrambled along the fiber length due to PMD. For sufficiently high PMD values, the GPON depletion tends to the average value calculated for random input SOP, that as shown in our previous paper [3] is given by $\langle A_{GPON}^{dB} \rangle = 1/2 A_{max}^{dB}$.

Finally, for very large PMD, the PDF of A_{GPON}^{dB} tends to become again deterministic, since the averaging of the SOP due to PMD is so high that the PDF is concentrated around its mean $\langle A_{GPON}^{dB} \rangle$, and the outage probability tends again to a 0/1 step function with a transition in:

$$P_{TWDM} \geq P_{TWDM}^{lim} = \frac{1}{10 \log_{10}(e) C_r L_{eff} N_{TWDM}}. \quad [\text{mW}] \quad (6)$$

which is 3 dB smaller than for the very low PMD case shown in Eq. 5.

Summing up, for co-polarized input SOPs, we expect a performance improvement in terms of P_{OOS} vs. P_{TWDM} as δ_{PMD} increases, since given a target P_{OOS} value, the maximum tolerable P_{TWDM} increases with δ_{PMD} .

3.2. Orthogonal input SOP

For orthogonal input SOP (Fig. 2(b)) and very low PMD, the PDF of the GPON depletion is concentrated around zero. This behavior is due to the fact that very low PMD practically maintains SOPs during propagation, and allows $\eta(L)$ in Eq. (2) to be considered as constant around zero and, consequently, P_{OOS} vs. P_{TWDM} is null for all reasonable value of P_{TWDM} , since the SRS effect is almost completely suppressed.

As PMD increases, performance in terms of P_{OOS} gets worse, since the GPON depletion PDF rapidly moves towards $\langle A_{GPON}^{dB} \rangle$. For sufficiently large PMD values, the GPON depletion follows the same behavior of the co-polarized case, as the propagation polarization scrambling allows considering the SRS induced depletion completely independent of the input SOPs.

3.3. DoP0 input SOP

The simulative PDF of the DoP0 configuration is omitted in Fig. 2. In fact we found that for such configuration, the PDF of the GPON depletion is a Dirac delta centered around $\langle A_{GPON}^{dB} \rangle$ for all practical PMD values, since the DoP of the TWDM-PON signals is set to zero at the transmitter, and this condition is maintained along the full fiber length. In fact, we observed that over the typical PON fiber lengths (i.e. up to 40 Km) and for all realistic PMD values, the N_{TWDM} channels maintain their relative state of polarization, since they are relatively closely spaced on a 100 GHz grid. In particular, the polarization decorrelation length [5] over some hundreds of GHz is of the order of hundreds of km, which is much larger than the fiber lengths in PON scenarios. In this condition, the GPON channel “sees” a completely depolarized set of TWDM channels along all the fiber lengths and, consequently, the SRS-induced depletion becomes almost deterministic, again around its average value, independently on the random

SOP of the GPON channel. The resulting P_{OOS} vs. P_{TWDM} function has thus again a threshold behavior, independent on the PMD value, so that $P_{OOS} = 0$ for all power levels smaller or equal than

$$P_{TWDM}^{lim} = \frac{1}{10 \log_{10}(e) C_{r,pol} L_{eff} N_{TWDM}} \quad [\text{mW}] \quad (7)$$

while for $P_{TWDM} \geq P_{TWDM}^{lim}$, $P_{OOS} = 1$.

3.4. Further comments on the consequences of different SOP launch

Some previous works on Raman and polarization effects made use of Gaussian assumptions on parameters such as A_{GPON}^{dB} . Observing Fig. 2 for the co-polarized and orthogonal cases, it appears anyway that the A_{GPON}^{dB} PDF differs from a Gaussian shape for relatively low PMD values. Considering for example Fig. 2(a), it is evident how the PDF is skew for $\delta_{PMD} < 0.02$ ps/ $\sqrt{\text{km}}$. Moreover, the resulting PDF strongly depends on the original SOP configurations. Such relatively low PMD regimes are anyway of practical interest as modern fibers installed for access networks may have PMD coefficients below 0.04 ps/ $\sqrt{\text{km}}$. This is thus the range of PMD values for which the results of this paper are completely new compared to the previously existing literature.

On the contrary, for medium-high PMD values, the PDF of A_{GPON}^{dB} can be reasonably approximated as Gaussian, since the polarization scrambling between GPON and TWDM-PON channels due to PMD is very large. Moreover, the PDF becomes almost independent of the original SOP configurations.

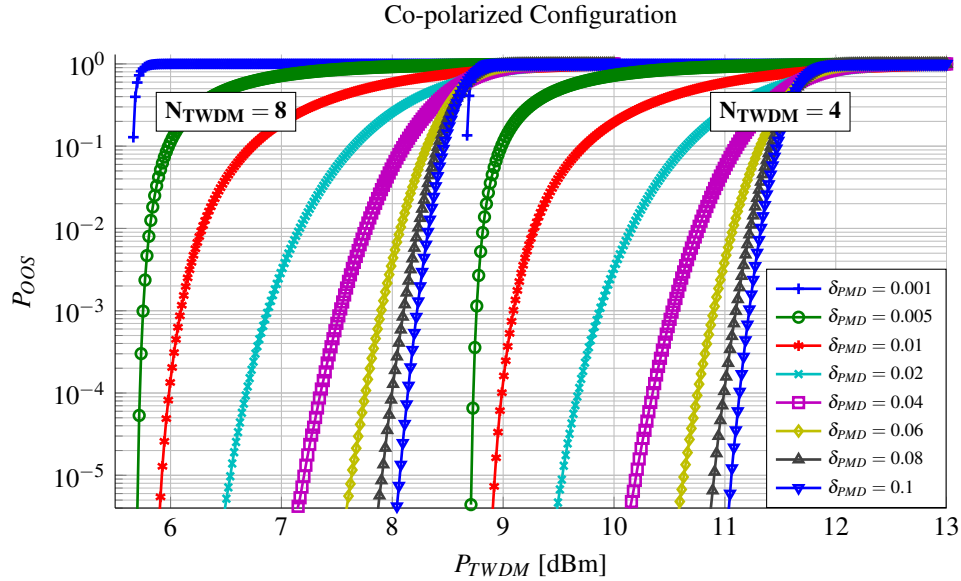


Fig. 3. P_{OOS} vs. P_{TWDM} for different values of δ_{PMD} for $L = 20$ km, for $N_{TWDM} = 4$ and $N_{TWDM} = 8$ and co-polarized configuration.

3.5. Out of service probability

We now start considering the outage probability in more details. We start showing Fig. 3 - 5, which depict the outage probability as a function of P_{TWDM} for the three considered launch con-

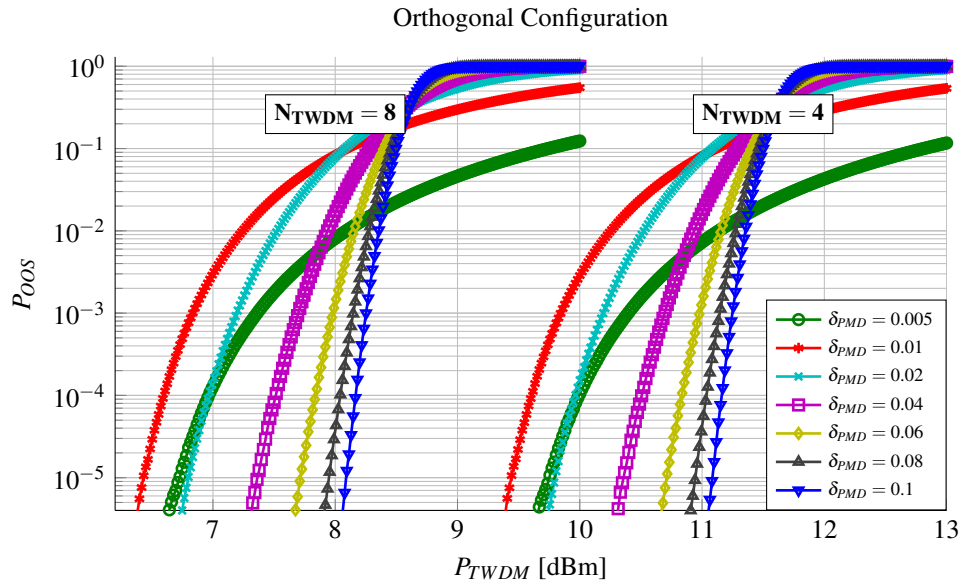


Fig. 4. P_{OOS} vs. P_{TWDM} for different values of δ_{PMD} for $L = 20$ km, for $N_{TWDM} = 4$ and $N_{TWDM} = 8$ and orthogonal configuration.

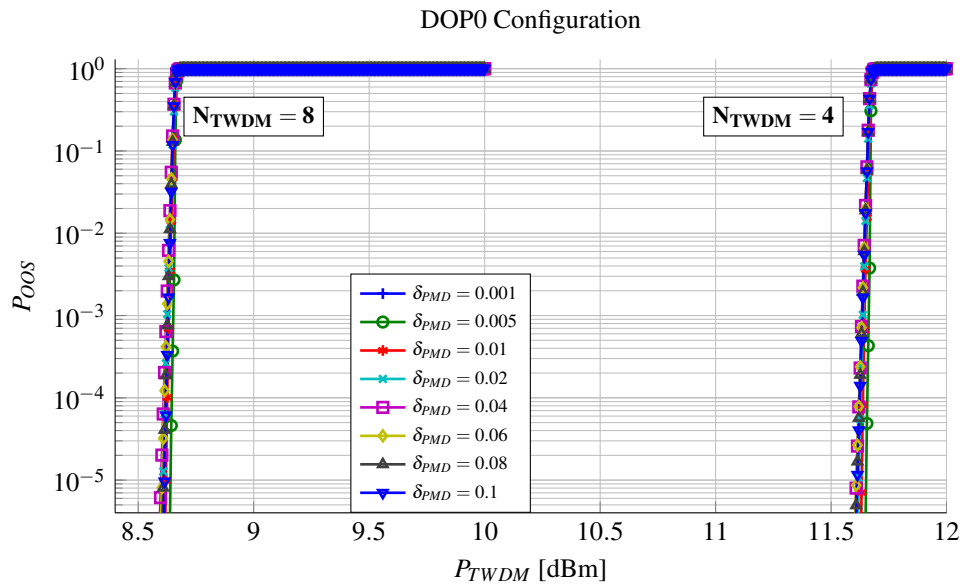


Fig. 5. P_{OOS} vs. P_{TWDM} for different values of δ_{PMD} for $L = 20$ km, for $N_{TWDM} = 4$ and $N_{TWDM} = 8$ and DOP0 configuration.

figurations, link length $L = 20$ km and different PMD values. Both $N_{TWDM} = 4$ and $N_{TWDM} = 8$ cases are shown in the same plot for each of configuration.

These curves shows numerically the trends that we anticipated in the previous section based on simple inspection of the simulative PDF curves but now some further comments can be made. We will explain the resulting trends for increasing PMD values.

- For co-polarized input SOP (Fig. 3), performance monotonically improves with δ_{PMD} .
- For orthogonal input SOP (Fig. 4) the results in terms of PMD are more difficult to be interpreted. In particular, when δ_{PMD} is almost zero (<0.001 ps/ $\sqrt{\text{km}}$ in our case) P_{OOS} is zero for all P_{TWDM} of interest, since the launch polarization orthogonality condition is preserved along the fiber length. As δ_{PMD} increases, performances rapidly worsen, since the PDF of A_{GPON}^{dB} starts showing an increasing average value and a significant skew and variance. In particular, increasing δ_{PMD} and due to the resulting PDF asymmetry, larger depletion values are more likely, inducing higher P_{OOS} for a given P_{TWDM} . As δ_{PMD} further increases, the A_{GPON}^{dB} PDF becomes symmetrical again, and its variance decreases, improving performances.
- Adopting the DOP0 launching scheme (Fig. 5) the outage probability has a stepwise behavior for all PMD values of interest, as can be readily derived by considering its PDF curves.
- In all cases, when comparing $N_{TWDM} = 4$ and $N_{TWDM} = 8$ performances in terms of P_{OOS} versus P_{TWDM} are worse for the latter case since GPON depletion is basically doubled.

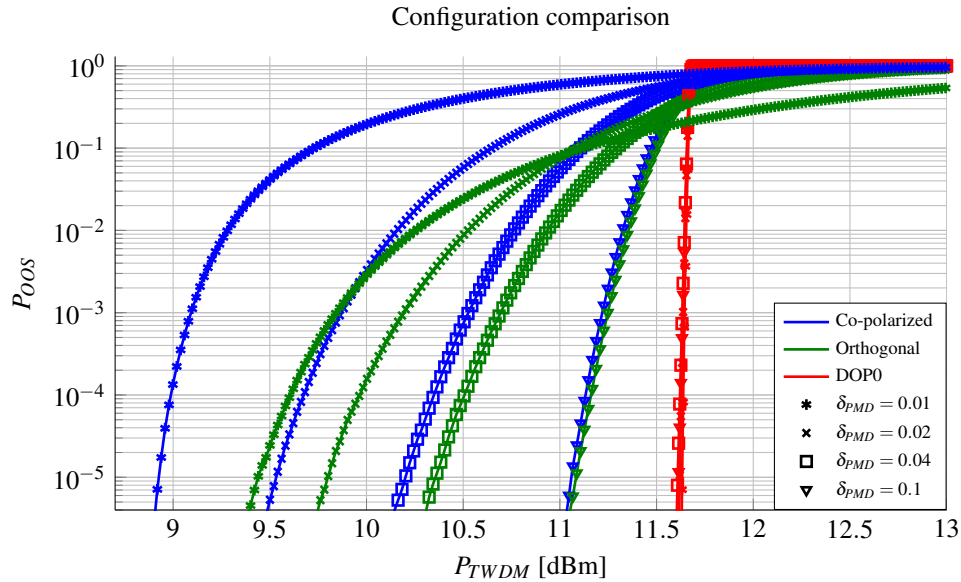


Fig. 6. P_{OOS} vs. P_{TWDM} for different values of δ_{PMD} for $L = 20$ km, for $N_{TWDM} = 4$ for all three different input SOP configurations.

In order to get a better insight on the consequences of different polarization launch conditions, we report in Fig. 6 the different results for 20 km link, $N_{TWDM} = 4$, and focusing only on some realistic PMD values. It is evident from the direct comparison of the different curves

P_{TWDM}^{max} vs L - $N_{TWDM} = 4$ - Target $P_{OOS} = 10^{-5}$

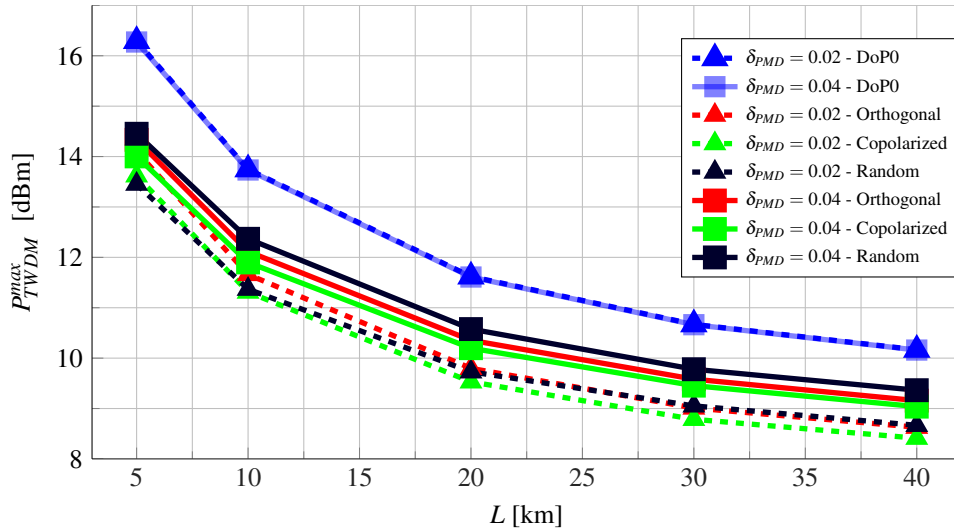


Fig. 7. Maximum admissible P_{TWDM} vs. δ_{PMD} for a target $P_{OOS} = 10^{-5}$ for $N_{TWDM} = 4$ and four different input SOP configurations, as a function of L

how the launching conditions can be very relevant on these out-of-service curves, at least for relatively low, but still realistic, PMD value. To summarize these issues, we plotted in the following Fig. 7 the maximum admissible power per TWDM-PON channel, called P_{TWDM}^{max} , able to guarantee an outage probability smaller than 10^{-5} as a function of the link length, for four different polarization launching schemes, $N_{TWDM} = 4$ and two different values of PMD. In this Fig. 7, the launching configuration with no polarization control is also shown for comparison. We labeled such launching scheme, described by the theory presented in [3], as “random”. The curves presented in Fig. 7 show some peculiar features and are likely the most important outcome of this paper, allowing deriving the following comments.

- For all the considered configurations, the maximum admissible power P_{TWDM}^{max} decreases as L increases
- The DoP0 configuration (blue curves) always has the best performances for all the considered values of δ_{PMD} and for all possible link lengths. Moreover, and very interesting from a practical point of view, the performance of such configuration is independent on the PMD value (which in a real installation are not precisely known). Additionally, such independence suggests that the same performances will be obtained independently on the input SOP of the GPON channel, provided that the TWDM-PON set has zero composite degree of polarization at the input. Thanks to such property, polarization control should be enforced only at the TWDM-PON transmitter, without considering the SOP of GPON, greatly reducing the complexity of polarization control.
- In the DoP0 case, the maximum admissible power can be up to 3 dB larger than the copolarized case, in particular for low PMD values. A gain for the DoP0 configuration in terms of P_{TWDM}^{max} is always present even with respect to all other conditions and PMD, even though it is smaller than 3 dB.

- The co-polarized configuration has the worst performance under all circumstances, whereas the orthogonal and the random ones stay in between the best and worst cases.
- As the link length and the PMD coefficient increase, the advantage of the DoP0 configuration over the other configurations decreases because the initial SOPs of the TWDM-PON and GPON channels become irrelevant due to the large polarization scrambling induced by PMD. However, for instance, for a link length of 40 km and $\delta_{PMD} = 0.04$ ps/ $\sqrt{\text{km}}$ the advantage of the DoP0 configuration with respect to the random case is still around 1 dB.

4. Fitting

In this section we present some heuristic numerical fitting on P_{TWDM}^{max} , which we believe is the main system parameter that is interesting to know in the scenario presented in this paper. We derive our results for both the DoP0 and the random configurations. Besides being able to deliver the best performance in terms of admissible maximum power for the TWDM-PON channels, such two configuration are also the most convenient in terms of backward compatibility with respect to the GPON standard since no polarization control is needed for that channel.

In short, the target of this section is giving a heuristic formula that fits the results presented in Fig. 7. For the DoP0 configuration, perfect agreement between the simulative results and Eq. (6) has been found so we can conclude that independently on PMD and target outage probability we have:

$$P_{TWDM}^{max,DoP0} = P_{TWDM}^{lim} = \frac{1}{10\log_{10}(e)C_rL_{eff}N_{TWDM}} \quad [\text{mW}] \quad (8)$$

For the random configuration, we looked for a fitting formula that introduces a penalty factor $K \in [0, 1]$ on the previous Eq. (8) thus modifying eq. (8) into the following:

$$P_{TWDM}^{max,rand} = \frac{K}{10\log_{10}(e)C_rL_{eff}N_{TWDM}} \quad [\text{mW}] \quad (9)$$

that in logarithmic units can be further simplified to:

$$P_{TWDM}^{max,rand} = P_{TWDM}^{max} + K_{dB} \quad [\text{dBm}] \quad (10)$$

In order to compute this penalty K_{dB} , a fitting algorithm based on the experimental data was used, obtaining the results of Fig. 8, which shows the original data and the fitted curves for four different values of PMD.

We saw that the fitting coefficient K_{dB} depends only on PMD, and thus we numerically evaluated its value as listed in Table 1, while we saw that it is constant for different loss coefficient α_{dB} . In order to verify this assumption, the K_{dB} calculations were repeated considering $\alpha_{dB} = 0.25$ and $\alpha_{dB} = 0.3$ dB/km. No meaningful variation in the penalty coefficient K_{dB} was found, meaning that all the variations in P_{TWDM}^{max} caused by variations of the fiber loss coefficient are already accounted for by the variation of the effective length L_{eff} in Eq. (8).

Table 1. Fit coefficient K_{dB} for the random case. This paramter can also be interpreted as the penalty in terms of P_{TWDM}^{max} between the random and the DoP0 cases.

δ_{PMD} [ps/ $\sqrt{\text{km}}$]	K_{dB} [dB]
0.01	-2.8
0.02	-2.1
0.04	-1.2
0.1	-0.5

P_{TWDM}^{max} vs L - $N_{TWDM} = 4$ - Target $P_{OOS} = 10^{-5}$ - Random Configuration

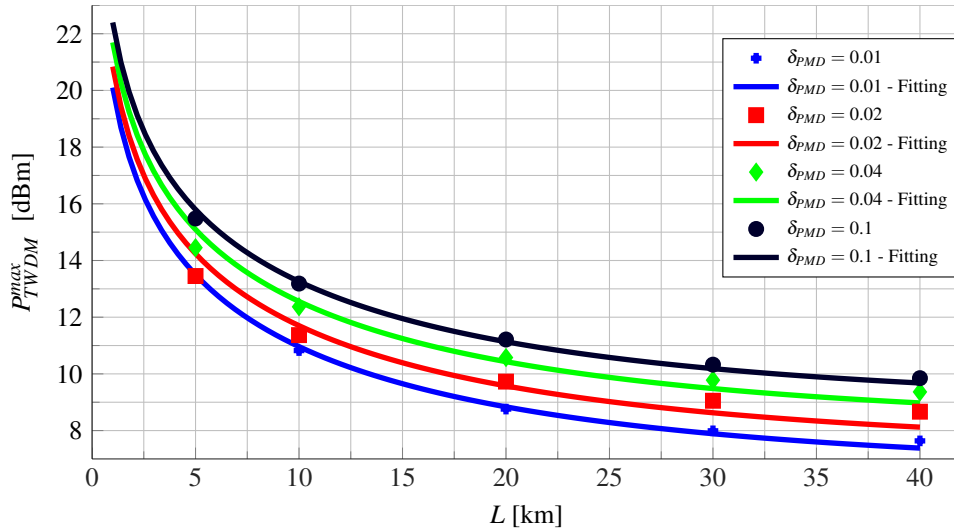


Fig. 8. Maximum admissible P_{TWDM} vs. δ_{PMD} for a target $P_{OOS} = 10^{-5}$ for $N_{TWDM} = 4$ and random input SOP configurations, as a function of L . Fitting curves also present.

The K_{dB} coefficient, being a penalty compared to the DoP0 case, decreases as the PMD increases due to the fact that the performance monotonically improves with PMD whenever the launch is either random or co-polarized [3]. Thanks to Tab.1, it is possible to quickly evaluate the advantage in terms of maximum transmittable power per TWDM-PON channel that is obtained by simply applying a fixed polarization configuration to the TWDM-PON channels. In this way, system designers can readily consider, depending on the link type, whether it is convenient or not, from a system perspective, to use polarization controllers for TWDM-PON channels.

5. Practical Design Rules and Conclusion

In this paper, a comparison between three possible input polarization configurations was performed, proving that when TWDM-PON channels are transmitted in the DoP0 configuration, the allowed power per TWDM-PON channel is maximized for any given outage probability target. Improvements of up to 2 dB for this DoP0 configuration with respect to all other practical configuration has been demonstrated for link with low PMD values (<0.02 ps/ $\sqrt{\text{km}}$). It should be said that for extremely (and unrealistically) low PMD links, orthogonal GPON/TWDM-PON polarization launching is in principle able to guarantee zero GPON SRS-induced depletion, but this potential advantage is quickly lost for realistic PMD values, and thus it has no practical interest.

For what concerns OLT TWDM-PON transmitters our paper thus shows that it may be interesting to implement a DoP0 polarization launch on the TWDM channels, which basically requires launching half of the TWDM channels on a given polarization, and the other half on the orthogonal one, without considering the SOP of the existing GPON channel. The OLT complexity to implement DoP0 clearly grows compared to the much more straightforward “random” launch of the N_{TWDM} channels, but we believe that such increase is actually worth considering in full co-existence scenario between TWDM-PON and all previous PON standards. A

DoPo implementation may in particular be relatively easily implemented in future TWDM-PON OLT using some integrated optoelectronic platforms. For instance, if all the TWDM-PON transmitters are integrated on a Silicon Photonics chip they will all have the same polarization inside the chip waveguides (that are intrinsically single-polarization) but then can be coupled on two orthogonal polarization modes in the output SMF fiber using 2D-grating structures.

Apart from the polarization related results, our paper also gives some very practical fitting functions to study the maximum amount of power that can be transmitted on the TWDM-PON channels as a function of several system parameters.

Acknowledgments

This work was partially carried out under the Italian funded PRIN research project “ROAD-NGN”. The authors would also like to thank Maurizio Valvo and his colleagues in Telecom Italia Lab for the fruitful discussion on the topics of this paper.